

New refined Model for Mechatronics design of solar differential drive mobile robotic platforms

Farhan A. Salem^{1,2}

¹ Dept. of Mechanical Engineering, Mechatronics Engineering Prog., College of Engineering, Taif University, 888, Taif, Saudi Arabia.

² Alpha center for Engineering Studies and Technology Researches, Amman, Jordan.

Email: salem_farh@yahoo.com

Abstract: *This paper proposes a new generalized and refined model for solar electric differential drive Mobile Robotic platforms (SEDDMRP) and some considerations regarding design, modeling and control solutions. The proposed system design consists of seven main subsystems, each subsystem, is mathematically described and corresponding Simulink sub-model is developed, then an integrated generalized overall model of all subsystems is developed. The proposed whole SEDDMRP system model is developed for research purposes and application in educational process, to help in facing the main challenges in developing Mechatronics SEV systems; early identifying system level problems and ensuring that all design requirements are met, also, it is developed to allow designer to have the maximum output data to select, evaluate and control the overall SEDDMRP system and each subsystem outputs characteristics and response, for desired overall and/or either subsystem's specific outputs, under various PV subsystem input operating conditions, to meet particular SEDDMRP system requirements and performance. The obtained results show the simplicity, accuracy and applicability of the presented models in Mechatronics design of SEDDMRP system application.*

Keywords: Mechatronics, Mobile Platform, differential drive, PV Panel, Modeling/simulation.

[1] Introduction

Modeling, simulation, analysis and evaluation process in Mechatronics design consists of two levels; sub-systems models and whole system model with various sub-system models interacting similar to real situation, the subsystems models and the whole system model, are to be tested and analyzed for desired system requirements and performance [1]. Mobile robot is a platform with a large mobility within its environment and have potential application in industrial and domestic applications. One of the simplest and most used structures in mobile robotics applications, are the two-wheel differential drive mobile robots shown in Figure 1(a)(b), it consists of a chassis with two fixed and in-line with each other electric motors and usually have one or two additional third (or forth) rear wheel(s) as the third fulcrum, in case of one additional rear wheel, this wheel can rotate freely in all directions, because it has a very little influence over the robot's kinematics, its effect can be neglected [2]. Solar electric mobile platform (SEMRP) system is relatively new field of mobile robots and new research area, different researches on Mobile robots fundamentals, applications, mathematical and Simulink models can be found in different texts including but not limited to in [1-14], most of it study separate specific system or subsystem design, dynamics analysis, control or specific application. A refined model of solar electric differential drive mobile robotic platforms (SEDDMRP) system that can represent the actual system kinematics and

dynamics, and that can be used in Mechatronics SEDDMRP system design is of concern.

To help in facing the main challenges in developing Mechatronics SEDDMRP systems; early identifying system level problems and ensuring that all design requirements are met, this paper extends writer's previous works [1-5][15-18] and proposes a new generalized and refined model for SEDDMRP systems and some considerations regarding design, modeling and control solutions. The proposed SEDDMRP system model consists of seven main subsystems, including; PV panel, DC/DC converter, PWM, battery, mobile platform, DC machine, control unit and differential drive kinematics and dynamics subsystems, each subsystem, is to be mathematically described and corresponding Simulink sub-model is to be developed, then an integrated generalized model of all subsystems is to be developed, the sub-models and whole system model, are to be developed to allow designer to have the maximum output data to select, evaluate and control the overall SEDDMRP system and each subsystem outputs characteristics and response, for desired overall and/or either subsystem's specific outputs, under various PV subsystem input operating conditions, to meet particular SEDDMRP system requirements and performance. The block diagram representation of proposed system configurations and control is shown in Figure 1(a)(b).

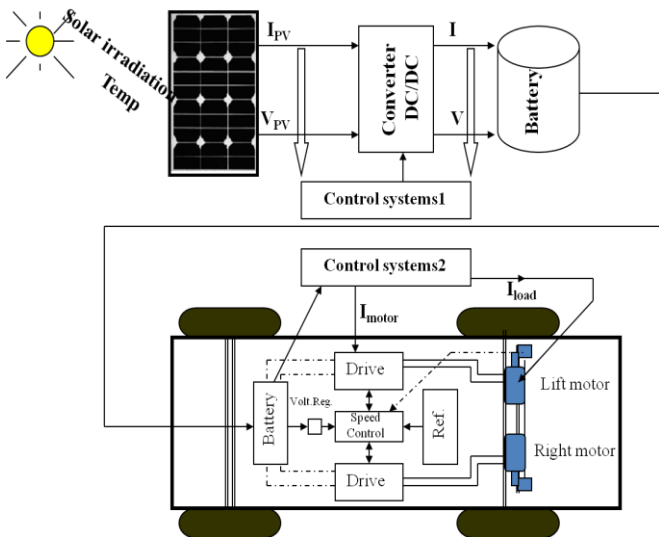


Figure 1(a) The block diagram representation of proposed system configurations and control

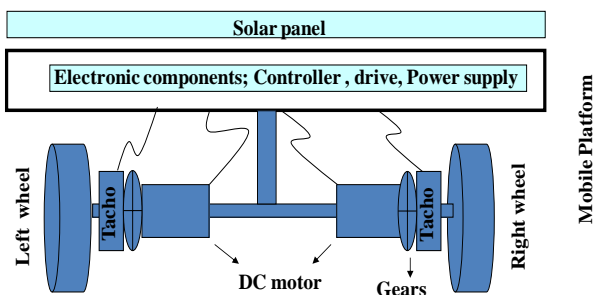


Figure 1(b) Components layout of SEDDMRP system

2. SEDDMRP system modeling

The proposed SEDDMRP system model consists of seven main subsystems, including; PV panel, DC/DC converter, battery, mobile platform, DC machine, control unit and differential drive kinematics and dynamics subsystems, each subsystem, is to be mathematically described and corresponding Simulink sub-model is to be developed, then an integrated generalized model of all subsystems is to be developed and tested. In [1-5][15-18] the refined mathematical models and corresponding Simulink sub-models of main subsystems are developed and tested, the modified versions of these sub-models will be used to develop the integrated and new generalized SEDDMRP system model.

2.1 Differential drive Kinematics and dynamics modeling.

Different resources can be found on modeling differential drive Kinematics and dynamics, including [2][19-22]. In [2] mathematical description of Differential drive Kinematics and dynamics is derived, Simulink model is developed and tested. To characterize the current localization of the mobile robot in its operational space of evolution in a 2D plane (x,y), first we must define its position and its orientation. Assuming the angular orientation (direction) of a wheel is defined by angle θ , between the instant linear velocity of the mobile robot v and the local vertical axis as shown in Figure 2(a). The linear instant velocity of the mobile robot v , is a result of the linear velocities of the left driven wheel v_L and respectively the right driven wheel v_R . These two drive velocities v_L and v_R are permanently two parallel vectors and in the same time, they are permanently perpendicular on the common mechanical axis of

these two driven wheels. When a wheel movement is restricted to a 2D plane (x,y), and the wheel is free to rotate about its axis (x axis), the robot exhibits preferential rolling motion in one direction (y axis) and a certain amount of lateral slip (Figure 2(a)(b)), the wheel movement (speed) is the product of wheel's radius and angular speed and is directly proportional by the angular velocity of the wheel, and given by Eq.(1):

$$(1) \quad \dot{x} = r\dot{\phi} \Leftrightarrow v = r\omega$$

Where: ϕ : wheel angular position. Referring to Figure 2(c), while the wheel is following a path and having no slippery conditions, the velocity of the wheel at a given time, has two velocity components with respect to coordinate axes X and Y and given as by Eq.(2):

$$r\omega = -v_x \sin \theta + v_y \cos \theta$$

$$0 = v_x \cos \theta + v_y \sin \theta$$

(2)

Assuming the mobile robot follows a circular trajectory shown in Figure 3, and Δs , $\Delta \theta$ and R are the arc distance traveled by the wheel, and its respective orientation with respect to the global coordinates, and R is the circumference radius of the wheel, then the linear and angular velocities of the mobile robot are given by Eq.(3):

$$v = \Delta s / \Delta t \Leftrightarrow \omega = \Delta \theta / \Delta t$$

(3)

The arc distance Δs traveled in time equal to Δt , is given by $\Delta s = R\Delta \theta$, and the *curvature*, that is the inverse of the radius R , is given by $\lambda = 1/R$, referring to Figure 3, the movement equation in the initial position are given by Eq.(4), these coordinate equations can be extended by their rotating, which result in Eq.(5), assuming the time is so small, then we have; $\cos(\Delta \theta) \cong 1$ and $\sin(\Delta \theta) \cong \Delta \theta$, substituting in Eq.(5), will result in Eq.(6):

$$\Delta x = R (\cos(\Delta \theta) - 1)$$

$$\Delta y = R (\sin(\Delta \theta))$$

(4)

$$\Delta x = R (\cos(\Delta \theta) - 1) \cos \theta - R \sin(\Delta \theta) \sin \theta$$

$$\Delta y = R (\sin(\Delta \theta) - 1) \sin \theta + R \sin(\Delta \theta) \cos \theta$$

(5)

$$\Delta x = -R \Delta \theta \sin(\theta)$$

$$\Delta y = R \Delta \theta \cos(\theta)$$

(6)

Substituting R , from the arc distance, $\Delta s = R\Delta \theta \Rightarrow R = \Delta s / \Delta \theta$, and dividing both sides by Δt , we have Eq.(7):

$$\Delta x = -\Delta s \sin(\theta) \Rightarrow \frac{\Delta x}{\Delta t} = \frac{-\Delta s \sin(\theta)}{\Delta t} \Leftrightarrow v_x = -v \sin(\theta)$$

$$\Delta y = \Delta s \cos(\theta) \Rightarrow \frac{\Delta y}{\Delta t} = \frac{\Delta s \cos(\theta)}{\Delta t} \Leftrightarrow v_y = v \cos(\theta)$$

(7)

2.1.1 The instantaneous center of curvature (ICC), (shown in Figure 2(a)) is the point the robot must rotate around it, to avoid slippage and have only a pure rolling motion, ICC lies on the common axis of the two driving wheels. In case of differential drive, by changing the velocities v_L and v_R of the two Left and Right wheels, the ICC of rotation will move and different trajectories will be followed, at each time Left and

Right wheels, moves around the ICC with the same angular speed rate, given by Eq.(8):

$$\omega = \frac{d\theta}{dt} \Leftrightarrow \omega R = v_{mob} \quad (8)$$

Referring to Figure 2(a) The right and left wheels linear velocities in terms of mobile angular speed are given by Eq.(9):

$$v_L = \omega_{mob} \left(R + \frac{L}{2} \right) \Leftrightarrow v_R = \omega_{mob} \left(R - \frac{L}{2} \right) \quad (9)$$

Where: R is the distance from the ICC point to the midpoint P , between the two wheels, and can be found by Eq.(10):

$$R = \frac{v_R + v_L}{v_R - v_L} * \frac{L}{2} \quad (10)$$

Because the vectors for linear speed of wheels v_L and v_R are orthogonal on the common axis of the driven wheels, we can write an equation to represent the angular velocity of the robot to be given by Eq.(11):

$$\omega = \frac{v_R - v_L}{L} = \frac{(\omega_R - \omega_L)r}{L} \quad (11)$$

The instant linear velocity of the mobile robot v_{mob} is attached and defined relative to the characteristic point P , this velocity is a result of the linear velocities of the left driven wheel v_L and respectively the right driven wheel v_R . These two drive velocities v_L and v_R are permanently two parallel vectors and, in the same time, they are permanently perpendicular on the common mechanical axis of these two driven wheels [23], and given by Eq.(12):

$$v_{mob} = \frac{v_R + v_L}{2} = \frac{(\omega_R + \omega_L)r}{2} \quad (12)$$

A differential drive mobile robot is very sensitive to the relative velocity of the two wheels, where: for $v_R = v_L$: then the radius R is infinite and the robot moves in a straight line. If $v_R = -v_L$: then the radius R is zero and the robot rotates around robot center point P (it rotates in place) . If $v_R \neq v_L$: The robot follows a curved trajectory around an ICC point located at a distance R from robot center point P .

The curvature, which is the inverse of the radius R is given by Eq.(13):

$$\lambda = \frac{1}{R} = \frac{\omega}{v_{mob}} = \frac{2}{L} * \frac{(v_R - v_L)}{(v_R + v_L)} \quad (13)$$

Now, substituting Eq.(12) in Eq.(7) , gives:

$$v_x = \frac{v_R + v_L}{2} \sin(\theta)$$

$$v_y = -\frac{v_R + v_L}{2} \cos(\theta)$$

The arc length, distance, traveled by the mobile robot, (point P) is the average of arcs lengths traveled by the two driven wheels and given by Eq.(14): :

$$\Delta S_L = (R + L/2)\Delta\theta \quad (14)$$

$$\Delta S_R = (R - L/2)\Delta\theta \Leftrightarrow \Delta S = (\Delta S_L + \Delta S_R) / 2$$

Correspondingly, the center orientation angle of the trajectory is given by Eq.(15) :

$$\Delta\theta = (\Delta S_L - \Delta S_R) / R \quad (15)$$

2.1.2 Odometry for differential drive

To derive the expressions for the actual position of the robot, referring to Figure 2(a), lets suppose that a differential drive robot is rotating around the point ICC with an angular velocity $\omega(t)$. During the infinite short time dt the robot center will travel the distance from the point $P(t)$ to $P(t+dt)$ with a linear velocity $V_{mob}(t)$. For infinite short time we can assume that the robot is moving along a straight line tangent in the point $P(t)$ to the real trajectory of the robot. Based on the two components of the velocity $V_{mob}(t)$, the traveled distance in each direction can be calculated [20]

$$\begin{aligned} dx &= v_x(t)dt \\ dy &= v_y(t)dt \end{aligned} \quad (16)$$

Substituting v_x and v_y from Eq.(7) , gives Eq.(17) :

$$\begin{aligned} dx &= v \sin(\theta(t))dt \\ dy &= v \cos(\theta(t))dt \end{aligned} \quad (17)$$

Similarly, the angular position can be found to be :

$$d\theta = \omega(t)dt \quad (18)$$

Integrating Eqs.(16,17) , substituting Eq.(7) and manipulating, we have Eq.(19) :

$$\begin{aligned} x(t) &= \int v \sin(\theta(t))dt + x_0 \\ y(t) &= \int v \cos(\theta(t))dt + y_0 \end{aligned} \quad (19)$$

$$\theta(t) = \int \omega(t)dt + \theta_0$$

Substituting Eqs.(12 and 14) and manipulating, we have Eq.(20) :

$$\begin{aligned} x(t) &= \int \left(\frac{v_R + v_L}{2} \right) \sin(\theta(t))dt + x_0 \\ y(t) &= \int \left(\frac{v_R + v_L}{2} \right) \cos(\theta(t))dt + y_0 \\ \theta(t) &= \int \frac{v_R - v_L}{L} dt + \theta_0 \end{aligned} \quad (20)$$

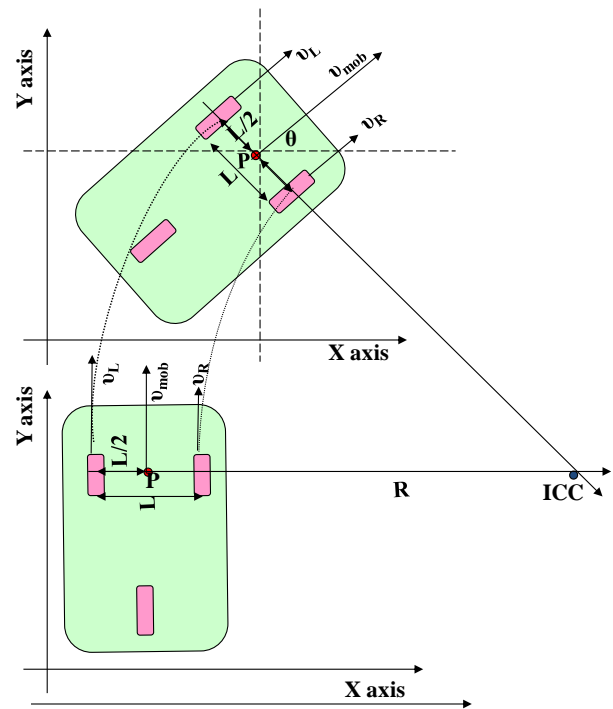


Fig.2(a) The differential drive motion

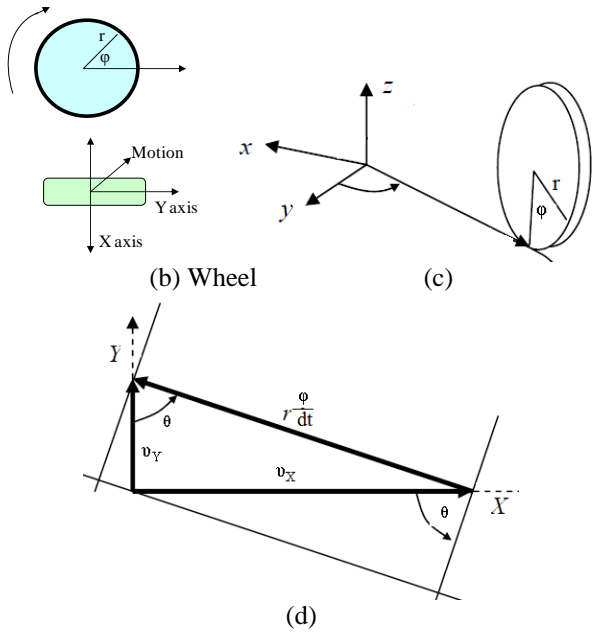


Figure 2(a)(b)(c) Wheel movement kinematics [2]

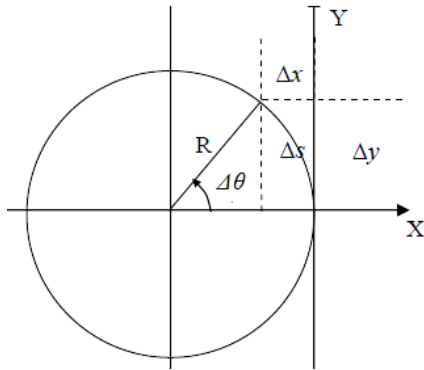


Figure 3 circumference movement of mobile robot [2]

2.2 Modeling of mobile platform dynamics

Different resources can be found on modeling of mobile platform dynamics, including [2,3,18][20-23]. In [2,3,18] a detailed derivation of refined mobile platform mathematical model and Simulink model considering most possible acting forces, are introduced, tested and verified.

The disturbance torque to mobile platform is the total resultant torque generated by the acting forces and given by Eq.(21), where and refereeing to Figure 4, the acting forces and torques on mobile platform include; the rolling resistance torque given by Eq.(22), The hill-climbing resistance, *slope*, torque, given by Eq.(23), the total inertia force of the mobile platform given by Eq.(24), the aerodynamics torque given by Eq.(25), the aerodynamics lift force, F_{lift} ; given by Eq.(26), the angular acceleration force, the force required by the wheels to make angular acceleration and is given by Eq.(27), the linear acceleration force F_{acc} , the force required to increase the speed of the SMEV and can be described as a linear motion given by Eq.(28).

To determine the electric battery capacity, and correspondingly design the Photovoltaic panel with series and parallel connected cells, it is required to estimated energy required by platform, the required power in kW that platform must develop at stabilized speed can be determined by multiplying the total force with the velocity of the SMEV, and given by Eq.(29): Electrical power (in watts) in a DC circuit can be calculated by multiplying current in Amps and V is voltage, and given by

Eq.(30). Based on fundamental principle of dynamics the acceleration of the vehicle is given by Eq.(31):

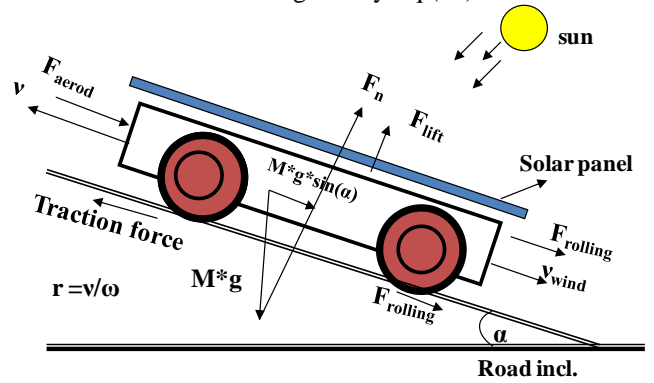


Figure 4. Forces acting on moving solar electric mobile robotic platform.

$$F_{Total} = F_a + F_R + F_C + F_{Lin_a} + F_{ang_a} \quad (21)$$

$$T_{rolling} = (MgC_r \cos(\alpha))r_{wheel} \quad (22)$$

$$T_{climb} = T_{slope} = (Mg \sin(\alpha))r_{wheel} \quad (23)$$

$$F_{inertia} = F_{slope} = M \frac{dv}{dt} \quad (24)$$

$$T_{aerod} = \left(\frac{1}{2} \rho A C_d v_{vehicle}^2 \right) r_{wheel} \quad (25)$$

$$F_{lift} = 0.5 \rho C_L B v_{vehicle}^2 \quad (26)$$

$$F_{acc_angle} = J \frac{n^2}{r_{wheel}^2} a \quad (27)$$

$$F_{acc} = M * a = M \frac{dv}{dt} = \left(M + \frac{J_{wheel}}{r^2} \right) \frac{dv}{dt} \quad (28)$$

$$F_{acc} = M * a = M \frac{d\omega}{dt} = M \frac{\sum T}{J} \quad (29)$$

$$P_{Total} = (\sum F) * v = F_{Total} * v \quad (30)$$

$$P = I \times V \quad (31)$$

$$\alpha = \frac{P_m - P_{total}}{M * v} \quad (31)$$

2.3 Actuator and Sensor subsystems modeling

In order to drive a SEMRP, induction motors, reluctance and permanent magnet motors can be used, the actuating machines most used in Mechatronics motion control applications are DC machines (motors), based on this, the SEDDMRP system motion control can be simplified to a DC machine motion control. In this paper, PMDC motor is considered as SEDDMRP electric actuator, depending on application requirements, any other actuating machine can also be used to replace DC motor to develop a generalized model [18]. In [1-4][14] introduced, tested and verified a detailed derivation of refined DC machine and tacho sensor systems' mathematical model and corresponding Simulink model, based on this, the open-loop transfer function of the DC machine is given by Eq.(31), In the following calculation the disturbance torque, T , is all torques including coulomb friction, and given by ($T = T_{load} + T_f$). Dynamics of tachometer can be represented using Eq.(32),

$$G_{open}(s) = \frac{\omega_{platform}(s)}{V_{in}(s)} = \frac{K_t/n}{(L_a s + R_a)(J_{equiv} s^2 + b_{equiv} s) + (L_a s + R_a)(T) + K_b K_t} \quad (31)$$

$$V_{out}(t) = K_{tach} \frac{d\theta(t)}{dt} \Rightarrow V_{out}(t) = K_{tach} \omega \Rightarrow K_{tach} = \frac{V_{out}(s)}{\omega(s)} \text{ and } \omega = \frac{V}{r} \quad (32)$$

2.4 Photovoltaic Panel and Converter (PVPC) subsystems modeling

In [15-16] a detailed derivation of mathematical model and corresponding Simulink model of both PV system and DC/DC converter systems are developed, tested and verified. In [16] a generalized Photovoltaic Panel –Converter (PVPC) subsystem model is developed, tested and verified, based on these references, the output net current I , of PV cell and the V-I characteristic equation of a PV cell are given by Eq.(33), it is the difference of three currents; the light-generated photocurrent I_{ph} , diode current I_d and the shunt current I_{RSH} . The output voltage, current and power of PV array vary as functions of solar irradiation level β , temperature T , cell voltage V and load current I .

Duty cycle is the ratio of output voltage to input voltage is given by Eq.(34), and defined as the ratio of the ON time of the switch to the total switching period, where: I_{out} and I_{in} : the output and input currents. In this paper, the PWM generator is assumed as ideal gain system, the duty cycle of the PWM output will be multiplied with gain $K_V = K_D$

$$I = I_{ph} - I_d - I_{RSH} \quad (33)$$

$$I = I_{ph} - I_s \left(e^{\frac{q(V+IR_s)}{NKT}} - 1 \right) - \frac{V + R_s I}{R_{sh}}$$

$$I = (I_{sc} + K_i (T - T_{ref})) \frac{\beta}{1000} - I_s \left(e^{\frac{q(V+IR_s)}{NKT}} - 1 \right) - \frac{V + R_s I}{R_{sh}} \quad (34)$$

$$\frac{V_{out}}{V_{in}} = D = \frac{I_{in}}{I_{out}} \Rightarrow V_{out} = D * V_{in} \Leftrightarrow D = \frac{T_{on}}{T_{on} + T_{off}}$$

2.5 Control algorithm subsystem selection and modeling

Different control approaches can be proposed to control the overall SEDDMRP system output performance in terms of output speed, as well as, controlling output characteristics and performance of PVPC subsystem to meet desired output voltage or current under input working operating conditions. Because of its simplicity and ease of design, PI controller is widely used in variable speed applications and current regulation, in this paper, different and separate PI controllers configurations will be applied for achieving desired outputs characteristics of both PVPC subsystem and SEDDMRP, and meeting desired output speed, voltage and load currents for particular SEDDMRP system application. The PI controller transfer function in different forms is given by Eq.(35).

$$G_{PI}(s) = K_p + \frac{K_I}{s} = \frac{(K_p s + K_I)}{s} = \frac{K_p \left(s + \frac{K_I}{K_p} \right)}{s} = \frac{K_p (s + Z_o)}{s} \quad (35)$$

$$G_{PI}(s) = K_{PI} * \frac{(T_I s + 1)}{T_I s} = K_{PI} * \left(1 + \frac{1}{T_I s} \right)$$

3. Proposed generalized SEDDMRP system model

The proposed generalized SEDDMRP system model shown in Figure 5 is developed by integrating all seven subsystems' sub-models to result in overall SEDDMRP system model, each subsystem's sub-model is designed and developed to return maximum output data (numerical visual and graphical) that can be used to select, evaluate and integrate sub-models output characteristics and performance as a part of the whole system performance, as well as, overall system performance. The proposed generalized model can have the design shown in Figure 5(b) where PV panel, converter and DC machine are modeled to represent platform's left side and wheel, and similarly, identical block to represent right side and wheel, the PV panel is modeled as two separate models to generate output voltage of 12 V.

The proposed generalized model is to be tested for *straight line, curvature, circular and motion profile motions*. to result in desired motion, a corresponding input signals must be applied to each or both actuators, for instant, for straight line motion the same input is to be applied to both actuator. To simulate different input values to both actuators, one (Figure 5(c)) or two ((Figure 5(b))) PV panels sub-model can be used in simulation (). To represent different motion types, a gain reduction or increasing Simulink block is to be used to send different inputs to different actuators, or to reduce output speed. It is important to notice that in microcontroller based mobile robots, a drive is used to drive DC motor and according to control program and applied PWM, each motor can be controlled separately, to move with specific speed and direction.

The desired output linear speed of SEDDMRP system is selected to be 1 m/s , for wheel radius $r = 0.075 \text{ m}$, the selected DC actuator is running at 12 DC input voltage, the tachometer constant K_{tach} , given by Eq.(32) and $\omega = v/r = 1/0.075 = 13.33 \text{ rad/s}$, correspondingly $K_{tach} = 12/13.33 = 0.9$.

The DC machine actuator sub-model is shown in Figure 6(a)(b), with corresponding *PI-armature-load-current* controller configurations and corresponding load torques given by Eqs.(21-29)

The PV panel subsystem sub-model is shown in Figure 7, this model can be used to represent a single PV cell, module, panel or array, it is required to define number of corresponding cells in series and parallel. PV panel can be modeled as two separate panels or one single panel, in case of single PV panel, it is to be designed to generate 24 V, where 12 V is required for each actuator, with series cells of $N_s = 96$ and parallel cell of $N_p = 30$,

The DC/DC buck converter subsystem sub-model is shown in Figure 8(a)(b), the desired output voltage is 24 V, half this value will be send to each DC machine. *The duty cycle* is calculated automatically by Eq.(36), both sub-models of PV panel and DC/DC converter are integrated in one PV panel-converter (PVPC) subsystem sub-model as shown in Figure 8(c).

$$D = \frac{V_{Conv_out_desired}}{V_{Panel_out}} \quad (36)$$

Control systems selection, design and simulation; Three separate PI control subsystems are used to control each of the following subsystems characteristics; PVPC subsystem output characteristics and platform subsystem output linear speed. For controlling the electric machine current and voltage a cascade strategy is applied where two separate current and speed controllers are used: *First PI speed* controller is used to control the platform linear speed to meet desired speed, and shown in Figure 6(b). The generalized model is also supported with other control algorithm including; PID, PD,PI with deadbeat response, and can be modified to include any other control strategy. *Second separate PI current* controller shown

in Figure 6(a) is used to match motor-current with required Load-Torque (Variations) current to overcome, where both currents are compared and the difference is fed to PI controller to generate output converter current to match required load current.

Third PI voltage controller shown in Figure 8(d), used to control the converter's output voltage to match desired output voltage, by comparing desired converter output voltage (12V) and actual converter's voltage, the difference is fed to PI controller to control the buck converter MOSFET switch according calculated duty cycle to result in desired voltage.

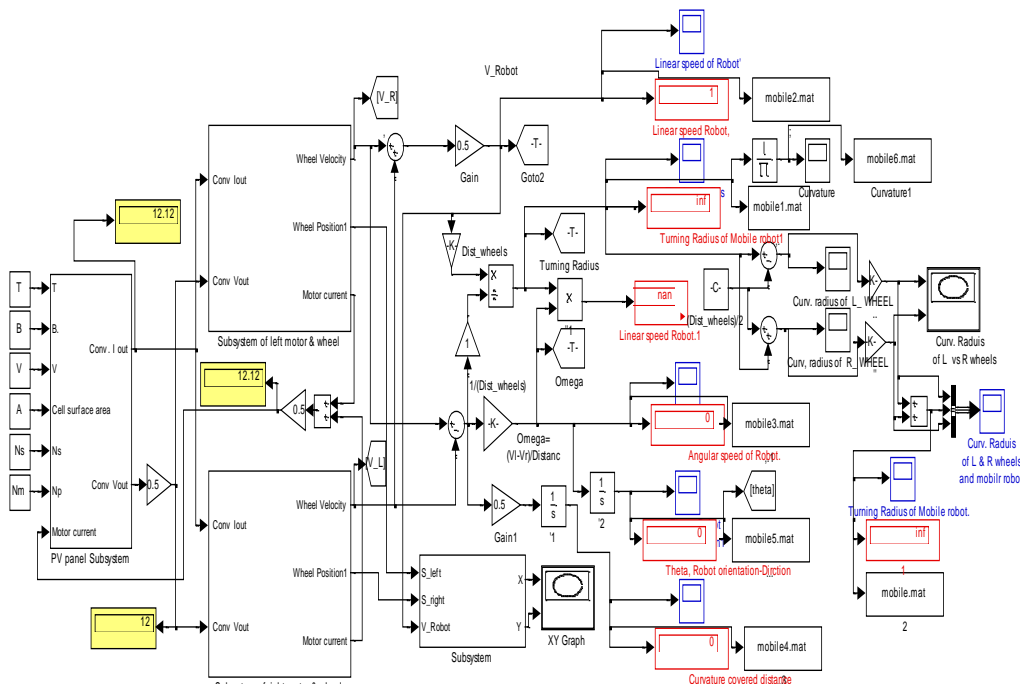


Figure 5(a) The proposed generalized SEDDMRP system model, with main subsystems; one PV panel, left motor, right motor and differential drive Kinematics and dynamics modeling

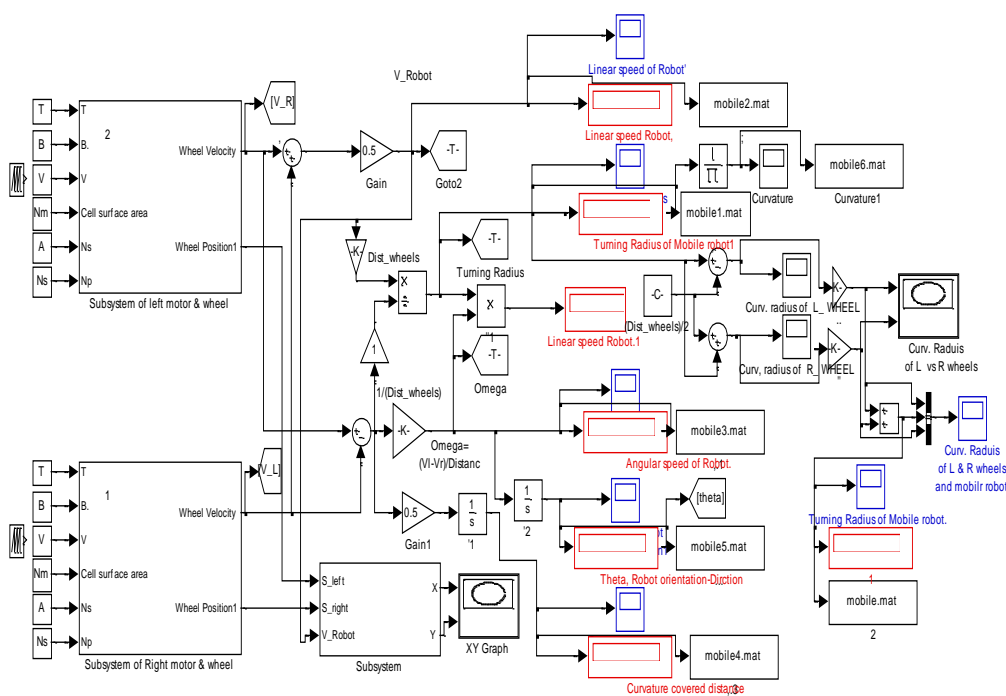


Figure 5(b) The proposed generalized SEDDMRP system model, with two mask sub-models, each with separate PV panel and converter connected to DC machine

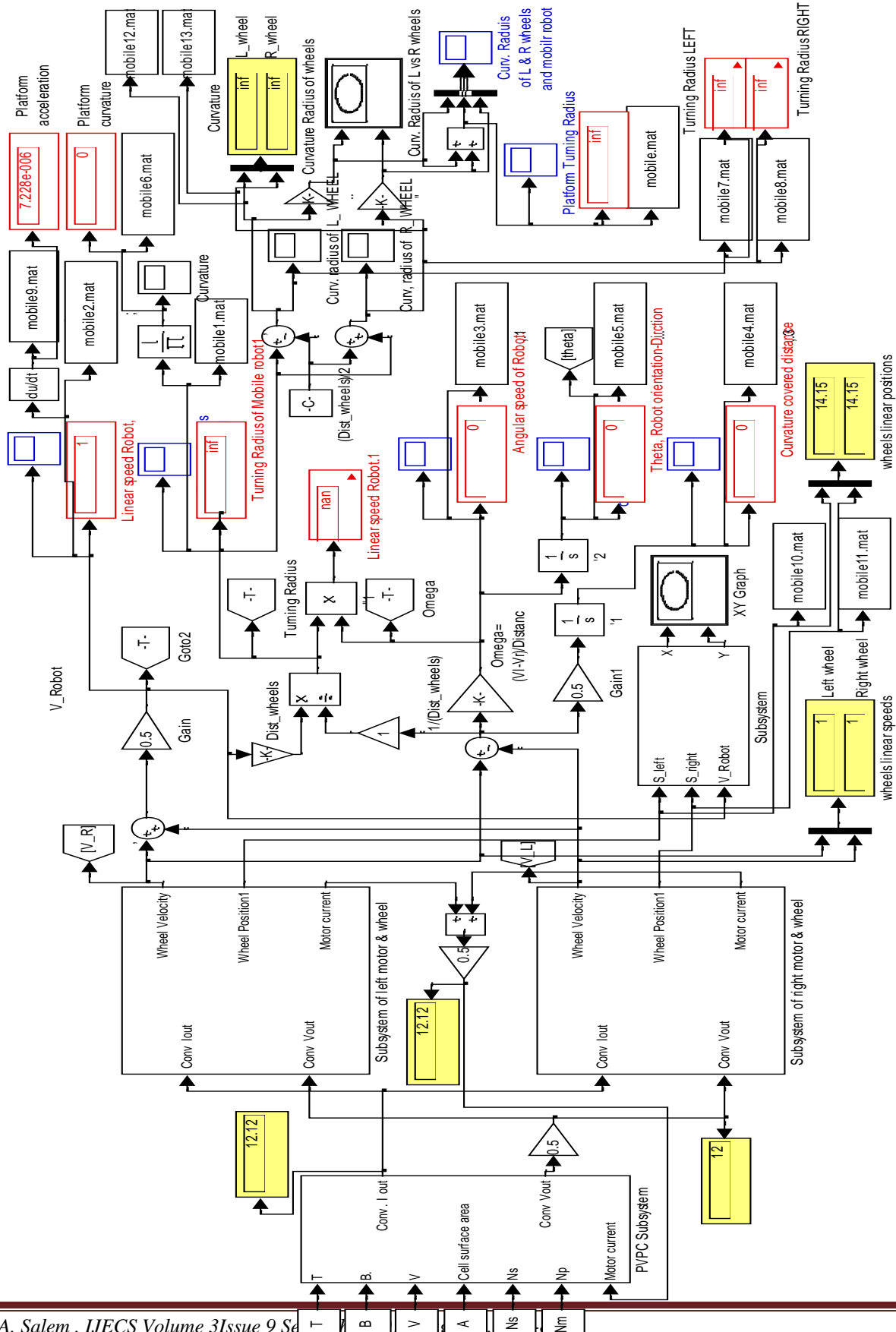


Figure 5(c) The proposed generalized SEDDMRP system model, with shown subsystems; one PV panel, left motor, right motor and differential drive Kinematics and dynamics modeling

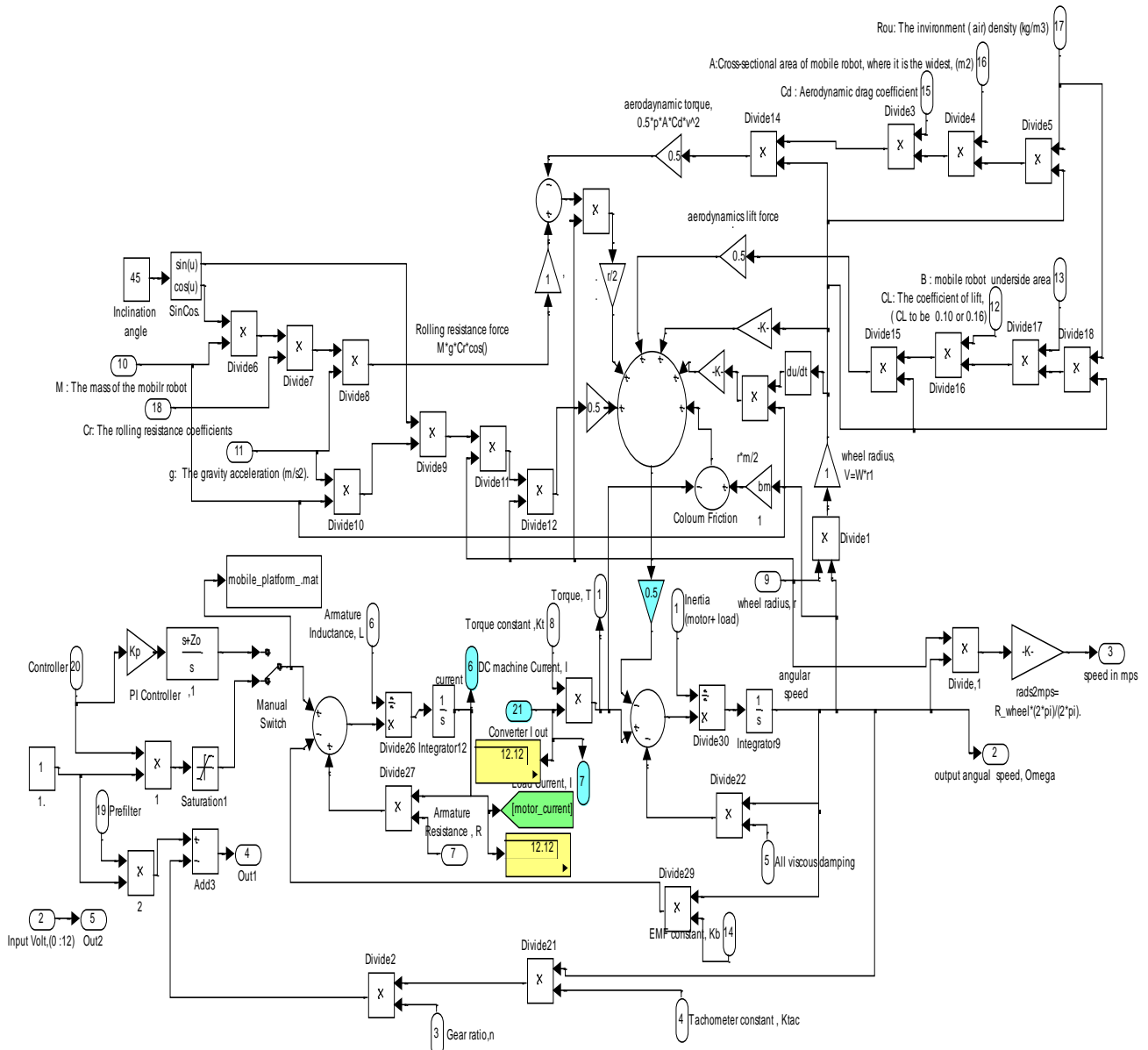


Figure 6(a) The DC machine sub-model, with PI-armature-load-current controller configurations, all shown as sub-model of generalized SEDDMRP model

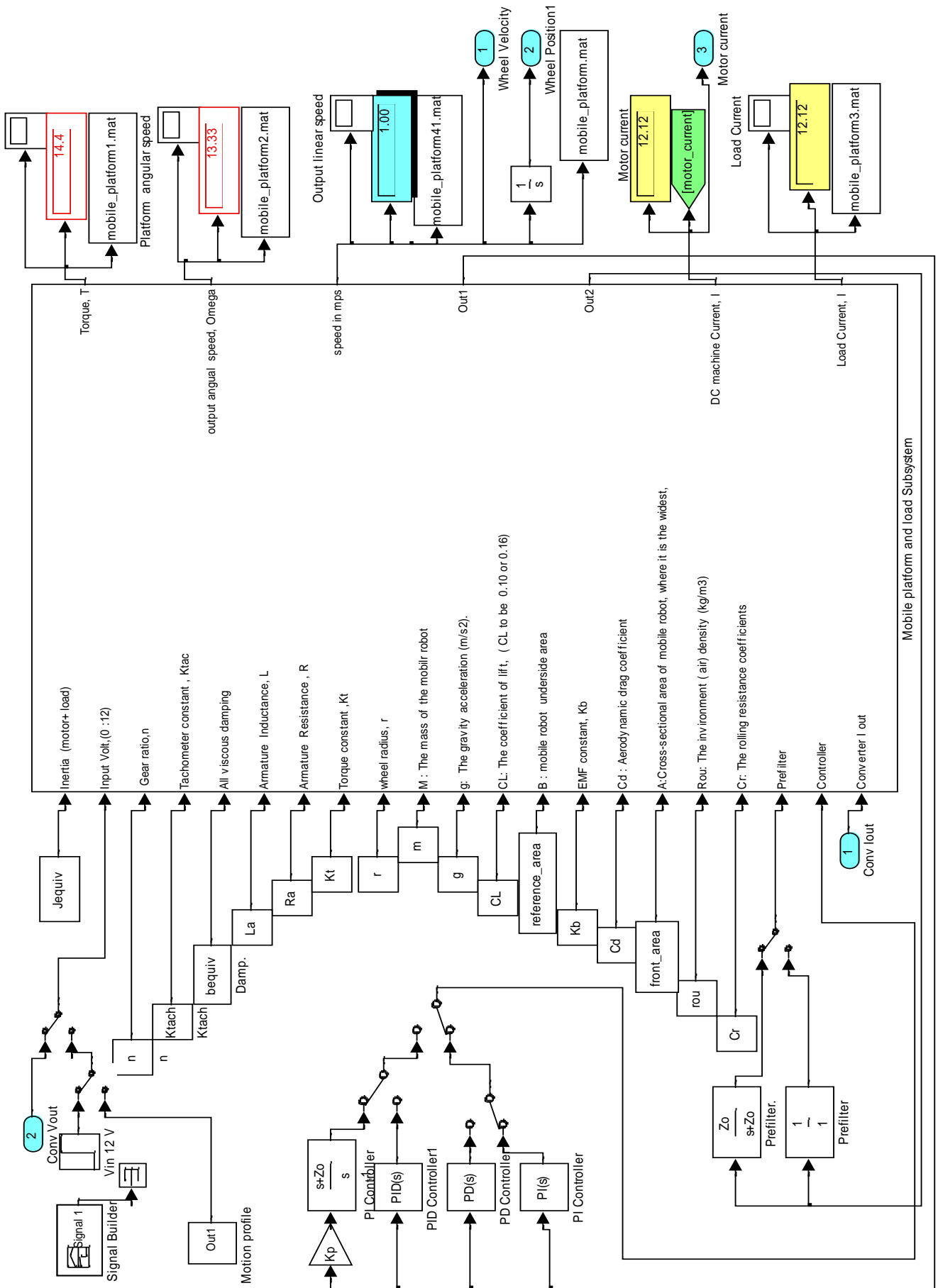


Figure 6(b) The DC machine mask sub-model, shown as sub-model of generalized model

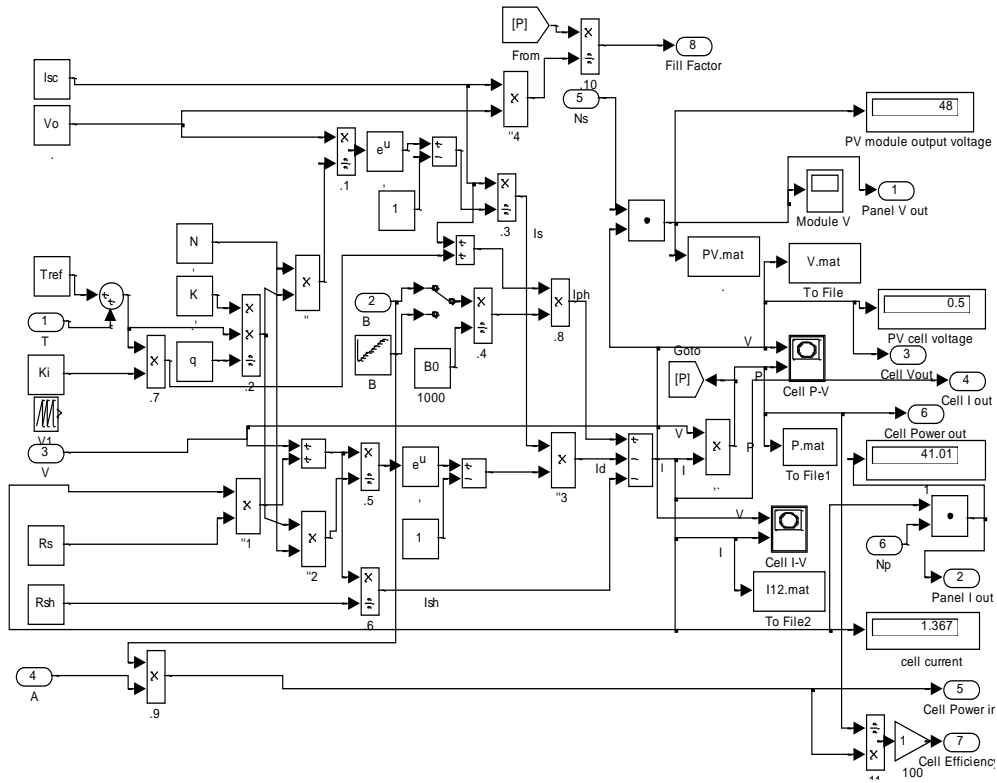


Figure 7 The PV panel subsystem sub-model

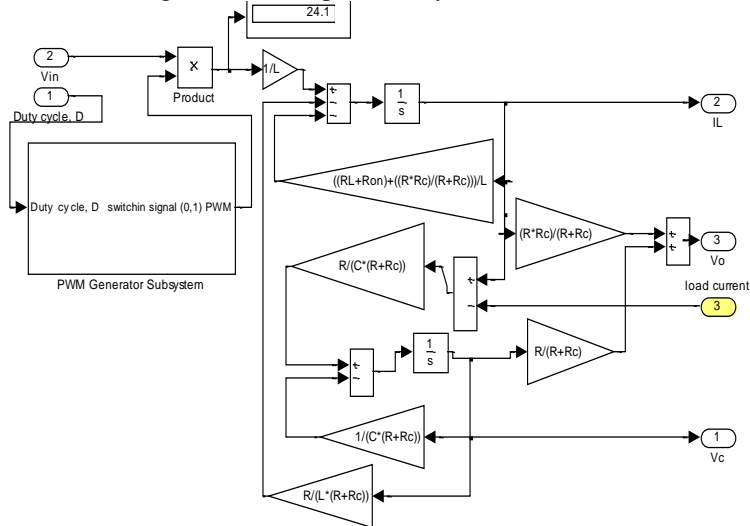


Figure 8(a) Buck converter subsystem sub-model, with PWM sub-model [24]

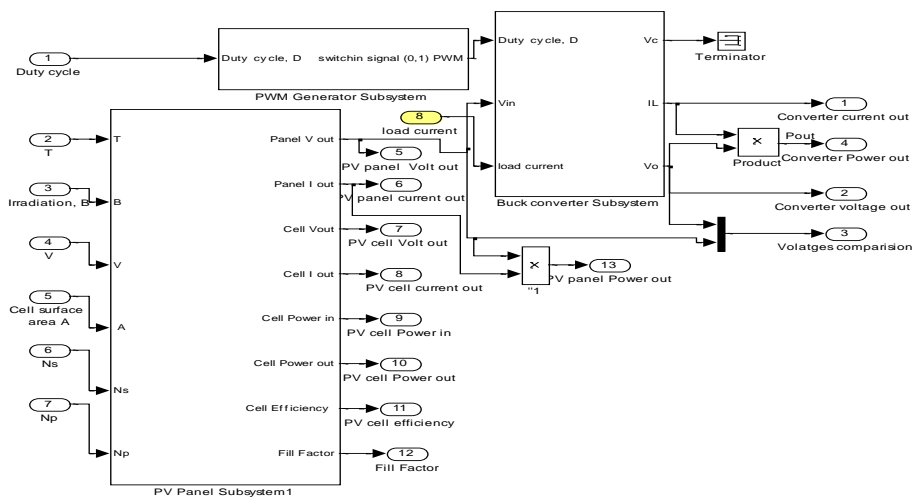


Figure 8(b) Mask sub-model of both PV panel and DC/DC converter sub-models

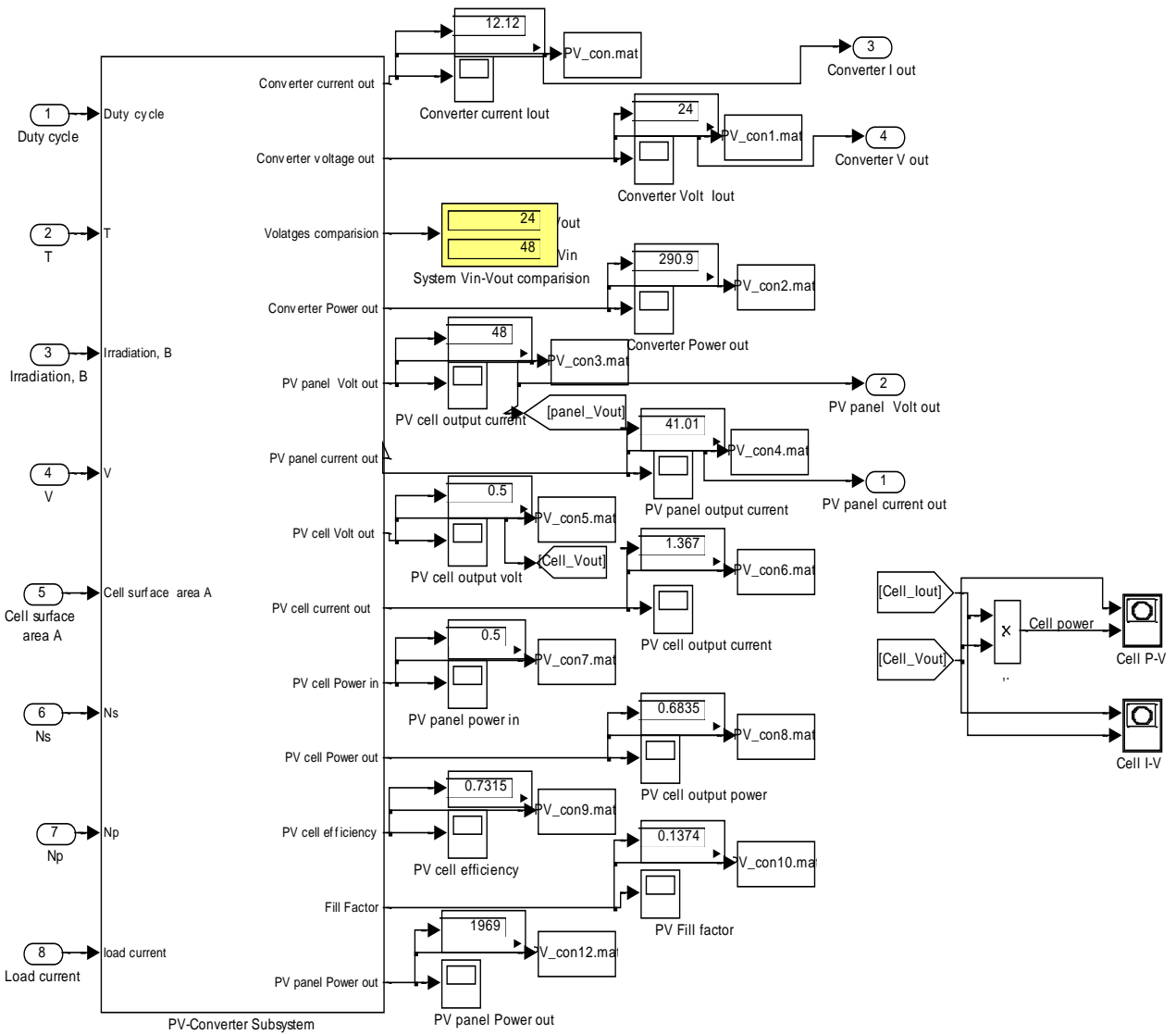


Figure 8(c) Mask sub-model of both PV panel and DC/DC converter sum-models

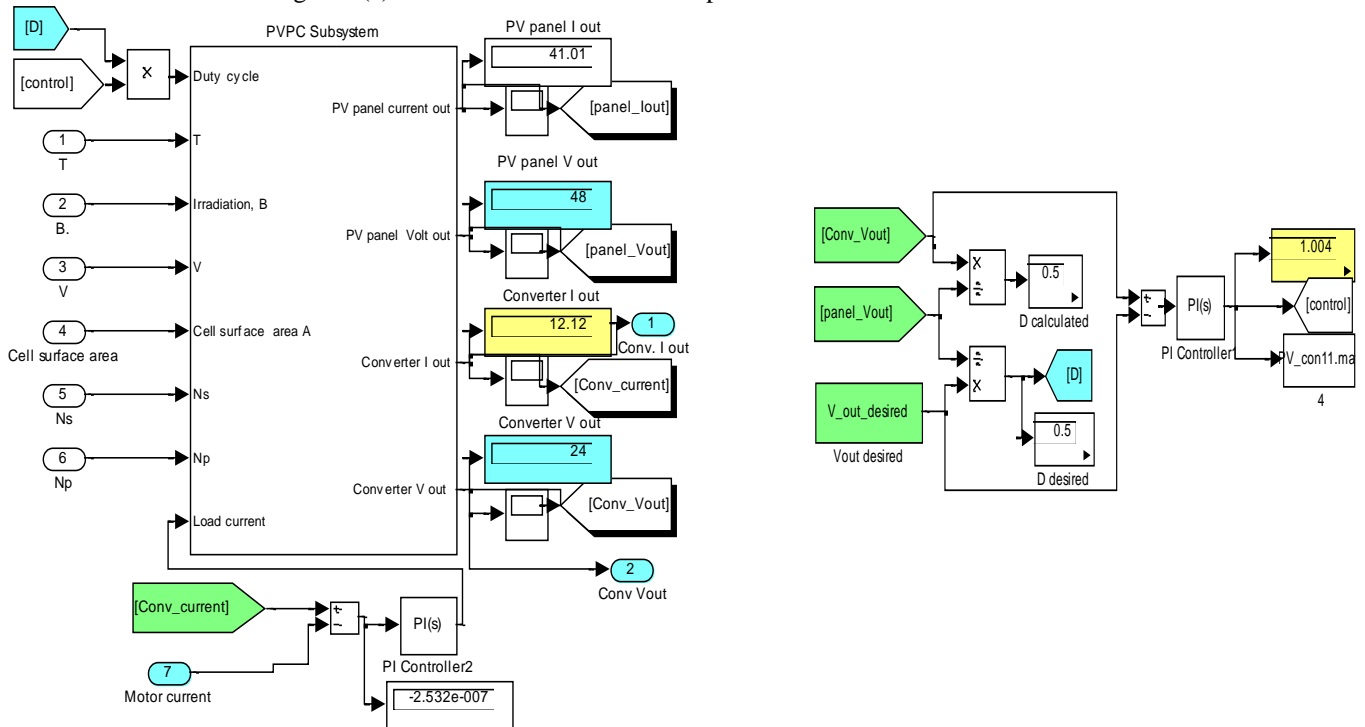


Figure 8(d) sub-models of; PV panel, DC/DC converter and PWM sub-models, with both PI controller for current and voltage control

4. Testing, analysis and evaluation

The proposed SEDDMRP system model is to be tested for output straight line, curvature, circular and motion profile motions, for defined subsystems parameters given in Table-3, and under PV panel input operating conditions of irradiation $\beta=200$, $T=75$, number of series and parallel cells $N_s=96$, $N_m=30$, cell surface area $A=0.0025\text{ m}^2$, and inclination of 45 degree.

The proposed model, is developed to return maximum required output numerical and graphical data of each subsystem and overall SEDDMRP system to be used to test, analyze and evaluate the SEDDMRP system performance and outputs characteristics including; Differential drive Kinematic and dynamic data; platform output linear speed, each wheel speed, position, acceleration, curvature, turning radius. DC machine outputs including; linear speed, acceleration, motor current, motor torque, load torque. PV cell-panel outputs, including; I-V, and P-V characteristics, current, voltage, power, efficiency, fill factor, and finally, DC/DC converter output including: current, voltage and Duty cycle value, tachometer constant.

4.1 Testing proposed generalized SEDDMRP system model for straight line motion,

Testing SEDDMRP model for straight line motion, will result in values numerically shown in each subsystem sub-model in all up Figures and listed in Table-1(a)(b). The output graphical data plots of PV panel output I-V, and P-V characteristics are shown in Figure 9(a)(b). The differential drive Kinematics and dynamics data including, platform and counterpoint linear speed of 1 m/s, platform linear acceleration, curvature, curvature covered distance, turning radius and wheels position, for straight line are shown in Figure 9(c)(d)(e). Left and right motors; linear speed, angular speed, torque and current, (both are identical) are shown in Figure 9 (d). PV panel-converter output voltages and output currents are shown in Figure 9(f). The control signals of PI speed and voltage controllers are shown in Figure 9(g), platform center point straight line motion is shown in Figure 9(e)

The proposed model is support with different control algorithms, any can be selected using manual switches, tested and evaluated. Selecting control PI-control algorithm with deadbeat response, designed according to design procedure given in [3-4], for desired output linear speed of 0.5 m/s, and straight line motion, will result in response curve shown in Figure 10.

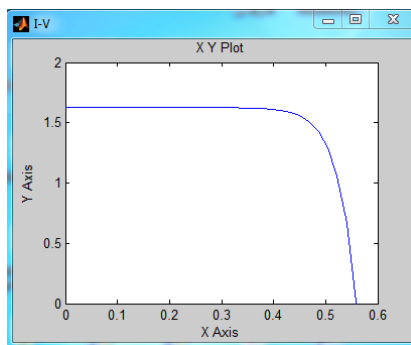


Figure 9(a) V-I Characteristics for $\beta=200$, and $T=50$

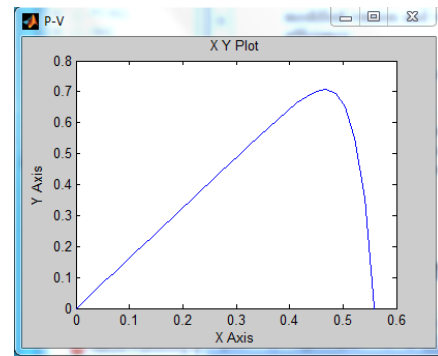


Figure 6 (b) P-V Characteristics for $\beta=200$, and $T=50$

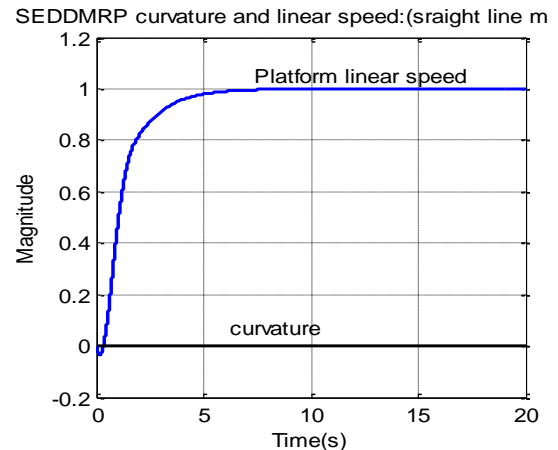


Figure 9 (c-1)

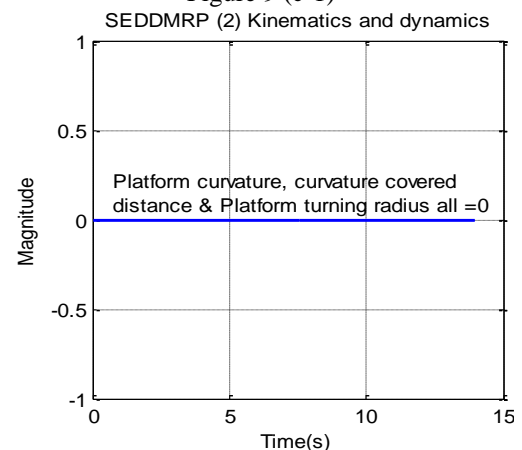


Figure 9 (c-2)

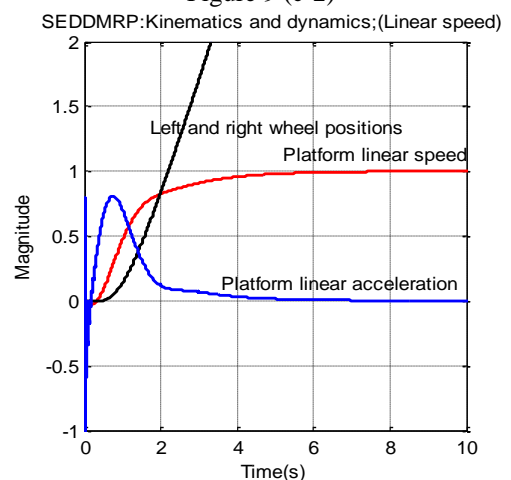


Figure 9 (c-3)

Figure 9 (c) Platform kinematics and dynamics ; linear speed, Platform's center point curvature, curvature covered distance and turning radius (zero) of SEDDMRP system for straight line motion

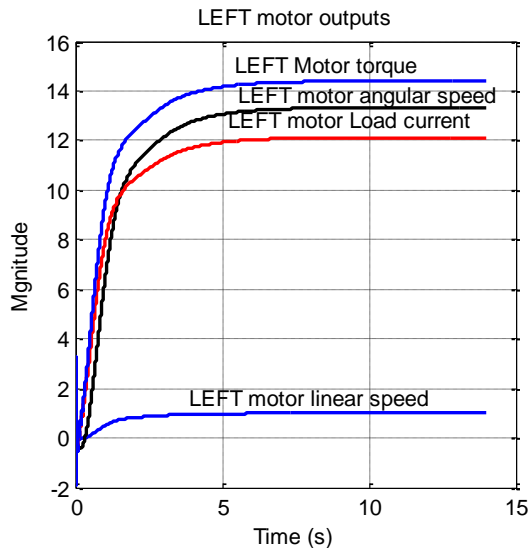


Figure 9(d-1)

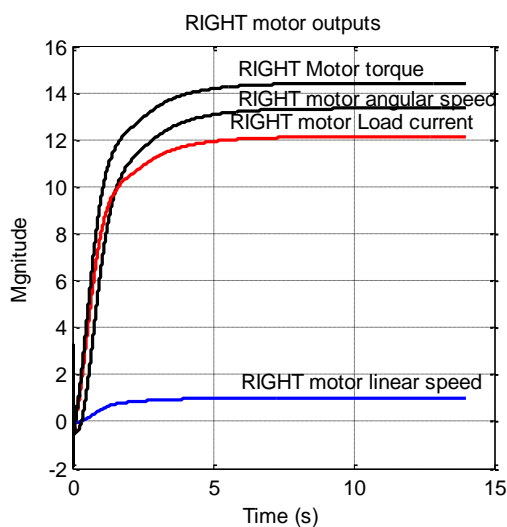


Figure 9(d-2)

Figure 9(d) left and right motors; linear speed, angular speed, torque and current, for straight line motion, (both are identical)

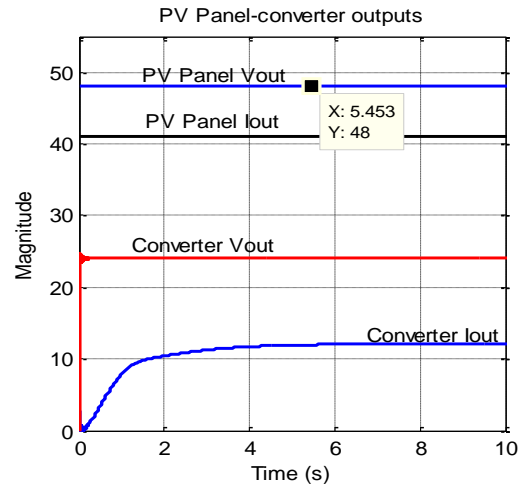


Figure 9(f) Panel-converter output voltages and output currents

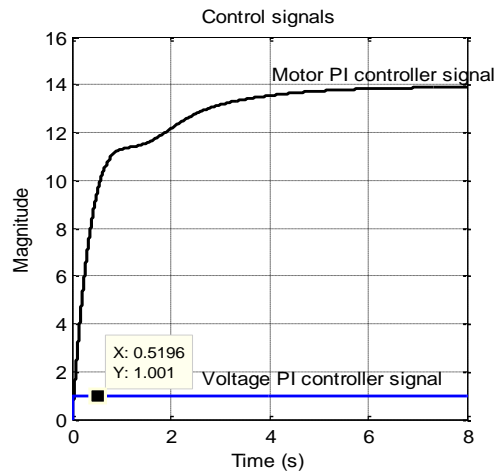


Figure 9(h) The control signals of PI speed and voltage controllers

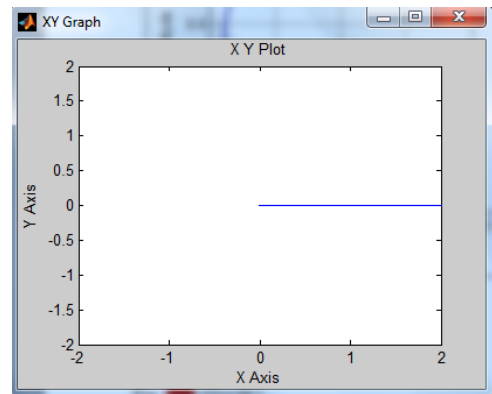


Figure 9(e) platform center point; Straight line motion

Table 1(a) Simulation results of each subsystem and whole SEDDMRP system for straight line motion

PVPC system inputs		PV cell outputs		PV Panel outputs		Converter outputs		Both DC machines outputs	
β	200	Voltage	0.5 V	Voltage	48 V	Voltage	24	Input voltage	12 V
T	75	Current	1.37 A	Current	41.01	Current	12.12	Shaft Angular. Speed.	13.33 rad/s
D	0.5	Fill factor	0.1374	Cell efficiency	1.277	Power out	290.9	Motor Torque	14.4 N/m ²
A	0.0025	Power out	0.6835	FF	0.1374			Motor current	12.12 A
N_s	96	Power in	0.5					Load current	12.12 A
N_p	30	Efficiency	0.7315						

Table 1(b) Simulation results of each subsystem and whole SEDDMRP system for straight line motion

Right Wheel outputs		left Wheel outputs		Platform outputs	
Linear Speed	1 m/s	Linear Speed	1 m/s	Linear speed	1 m/s
Curv. radius	0	Curv. radius	0	Curvature	0
Curvature	0*	Curvature	0*	Angular. Speed.	0
Lin. Position	13.9	Position	13.9	Orient. direction	0
				Turning radius	0
				Curvature covered distance	0

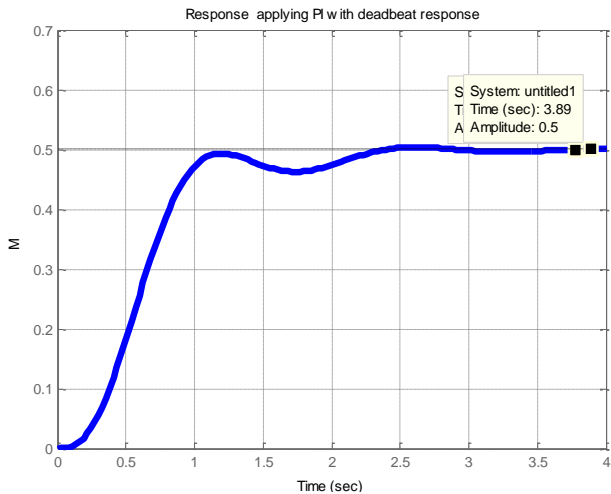


Figure 10 linear speed vs. time applying PI-control algorithm with deadbeat response, for desired output linear speed of 0.5 m/s, and straight line motion

4.2 Testing for circular motion

Testing SEDDMRP model for circular motion, will result in output numerical and graphical outputs values of each subsystem sub-model and overall system response shown in Figures 11(a), and listed in Table-2(a)(b), as well as, graphical outputs and responses shown in Figures 11, including outputs of ; PV panel, converter, DC machines, right and left motors, and overall SEDDMRP system.

The output graphical data plots of PV panel output I-V, and P-V characteristics are the same as shown in Figure 11(b). The differential drive Kinematics and dynamics data including, platform and counterpoint linear speed of 1 m/s, platform linear acceleration, curvature, curvature covered distance, turning radius and wheels position, for straight line are shown in Figure 11(b-i). Left and right motors; linear speed, angular speed, torque and current, are shown in Figure 11(f). PV panel-converter output voltages and output currents are shown in Figure 11(g). The control signals of PI speed and voltage controllers are shown in Figure 11(h), platform center point circular motion is shown in Figure 11(i). Testing SEDDMRP model for double curvature motion is shown in Figure 12.

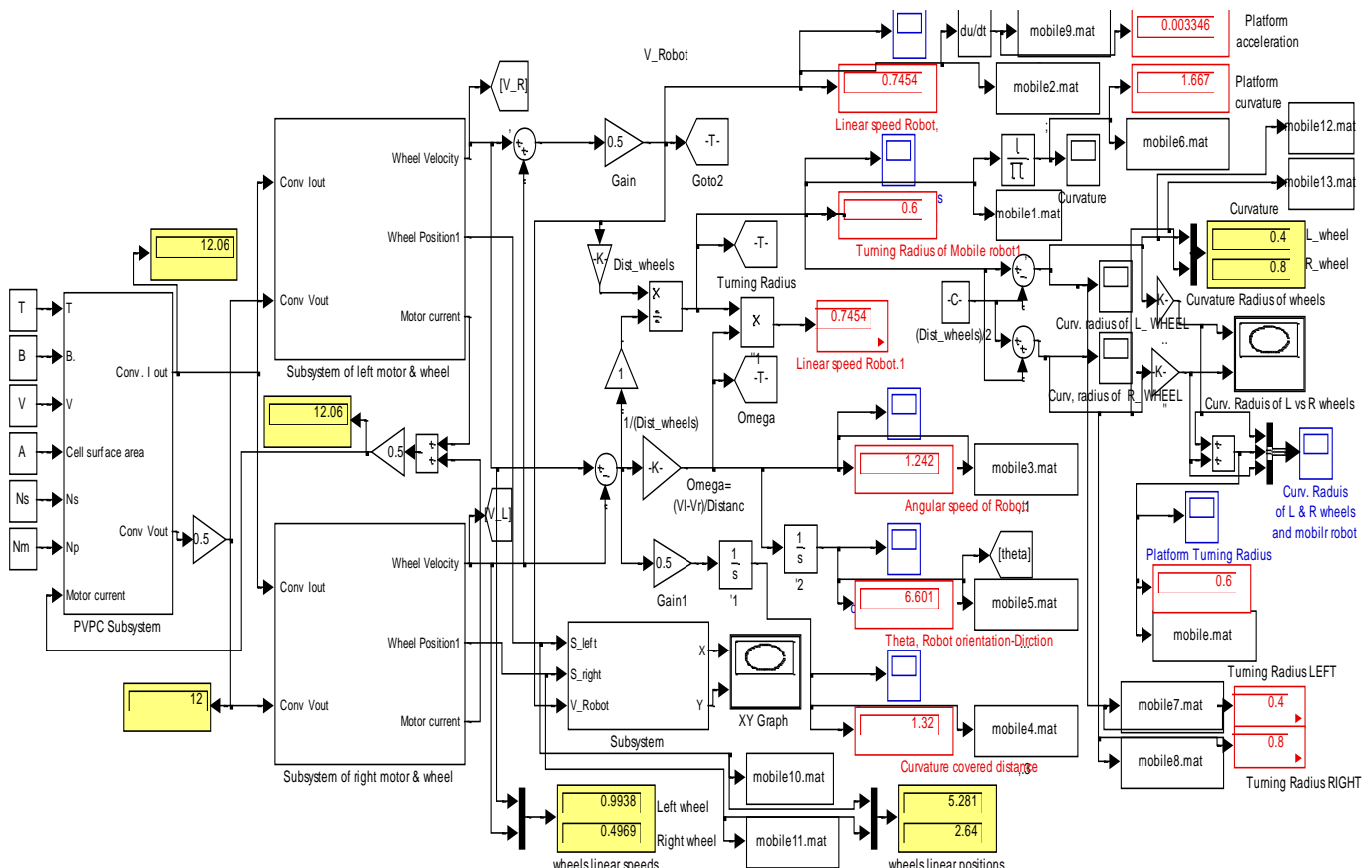


Figure 11(a) Testing model for circular motion

Table 2(a) Simulation results of each subsystem and whole SEDDMRP system for straight line motion

PVPC system inputs		PV cell outputs		PV Panel outputs		Converter outputs		Right DC machine outputs	
β	200	Voltage	0.5 V	Voltage	48 V	Voltage	24	Input voltage	12 V
T	75	Current	1.37 A	Current	41.01	Current	12.12	Shaft Angular. Speed.	13.33 rad/s
D	0.5	Fill factor	0.1374			Power out	290.9	Motor Torque	14.4 N/m ²
A	0.0025	Power out	0.6835					Motor current	12.12 A
N_s	96	Power in	0.5					Load current	12.12 A
N_p	30	Efficiency	0.7315						

Table 2(b) Simulation results of each subsystem and whole SEDDMRP system for straight line motion

Left DC machine outputs		Right Wheel outputs		left Wheel outputs		Platform outputs	
Input voltage	12 V	Linear Speed	0.5 m/s	Linear Speed	1 m/s	Linear speed	0.75 m/s
Shaft Angular. Speed.	6.665 rad/s	Curv. radius	0.4	Curv. radius	0.8	Curvature	1.667
Motor Torque	14.4 N/m ²					Angular. Speed.	1.25 rad/s
Motor current	12.12 A					Orient. direction, θ^* for t	23.22
Load current	12.12 A					Turning radius	0.6
						Curvature covered distance * for t	4.655 m

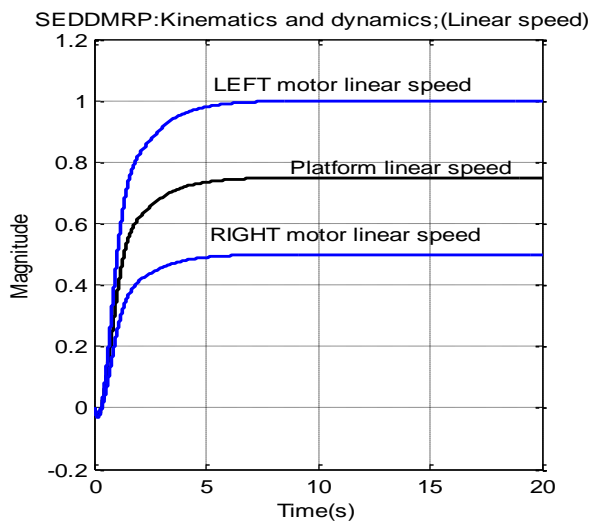


Figure 11(b-1)

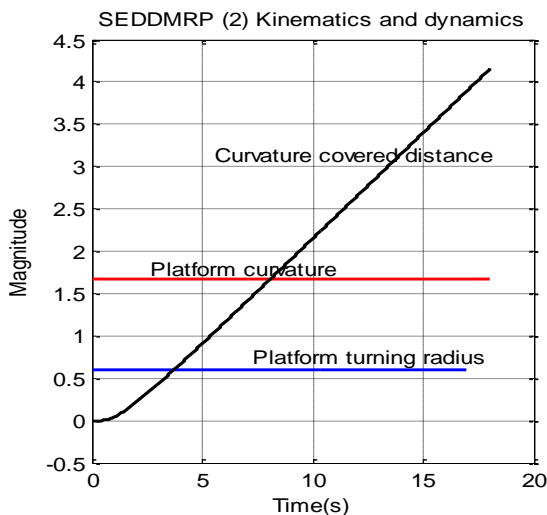


Figure 11(b-2)

Figure 11(b) Platform Kinematic and dynamic analysis, including; curvature, turning radius, covered curvature distance, platform linear speed and speed of right and left wheels

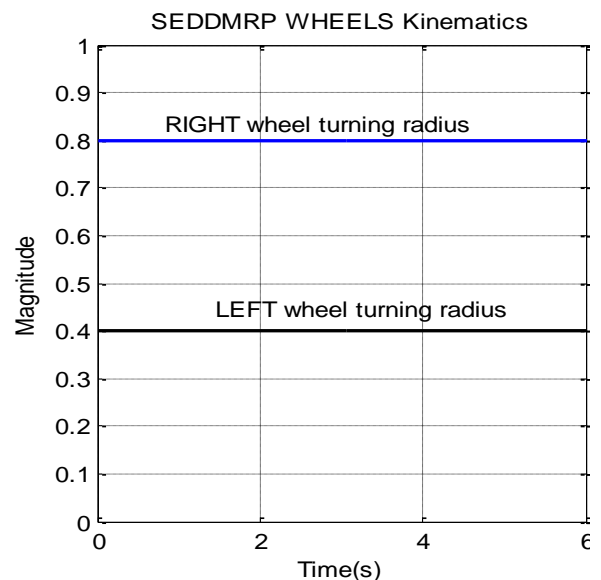


Figure 11(c-1)

SEDDMRP:Kinematics and dynamics (Angular speed)

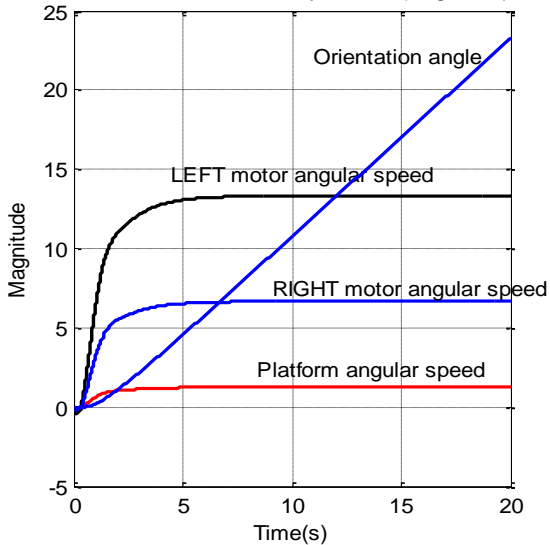


Figure 11(c-2)

Figure 11(c) Platform Kinematic and dynamic analysis; left and right motor turning radius, angular speed, orientation angle, and platform angular speed

Figure 11(d) Platform Kinematic and dynamic analysis; left and right wheel positions, platform curvature, platform turning radius, curvature covered distance

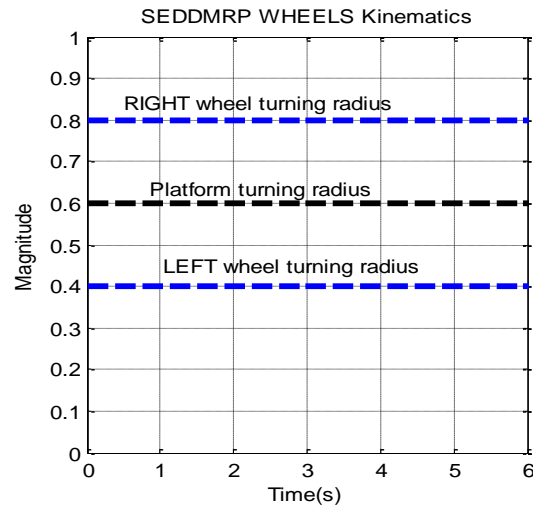


Figure 11(e) Platform Kinematic and dynamic analysis, right and left wheels and platform turning radius

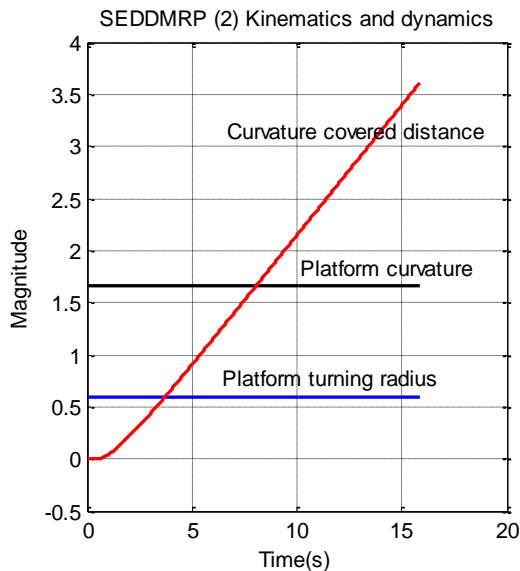


Figure 11(d-1)

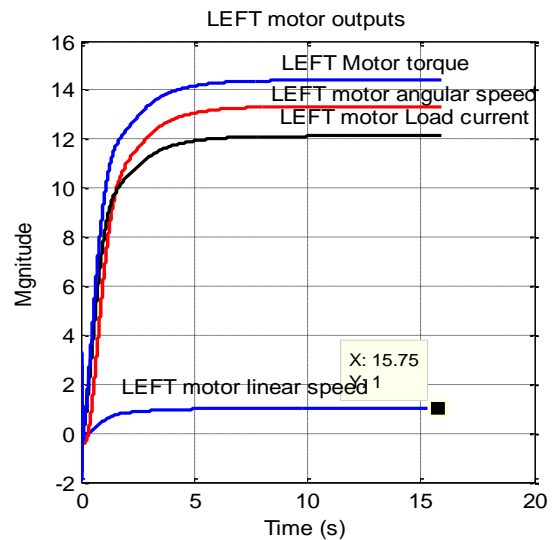


Figure 11(f-1)

SEDDMRP:Kinematics and dynamics;(wheels position)

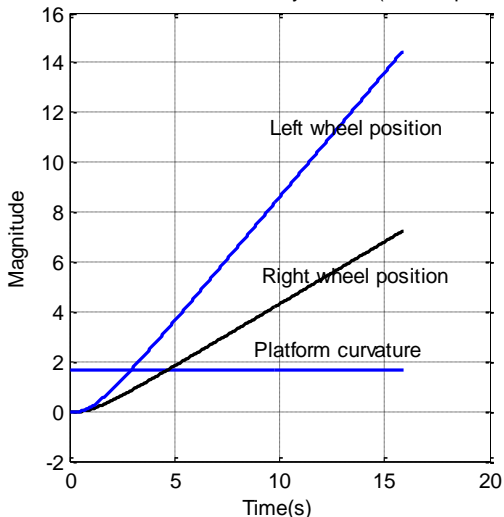


Figure 11(d-2)

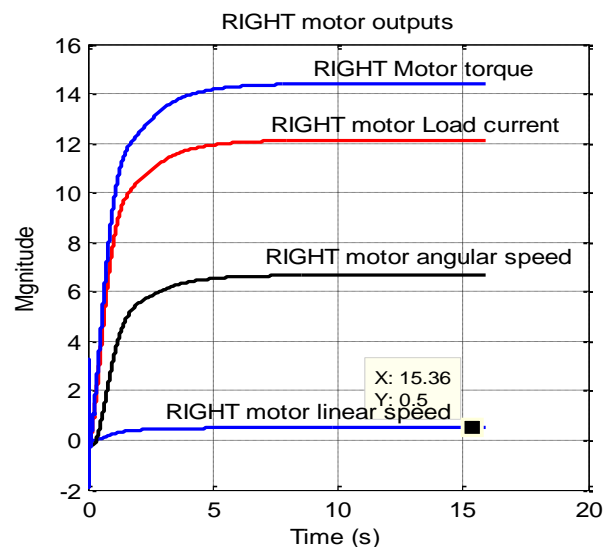


Figure 11(f-2)

Figure 11(f) Right and left motor outputs; linear speed, torque, and angular speed

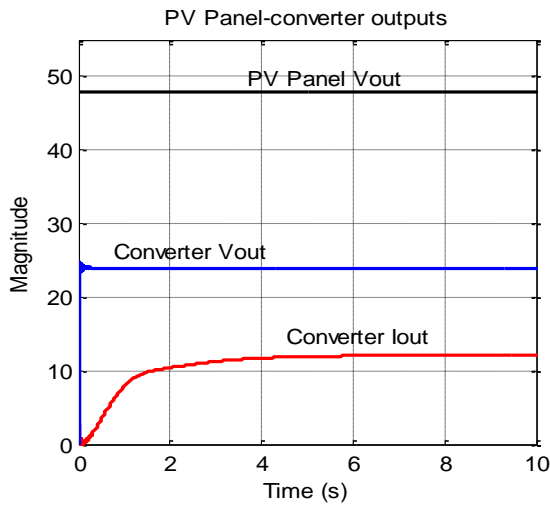


Figure 11(g) Panel-converter output voltages and output currents

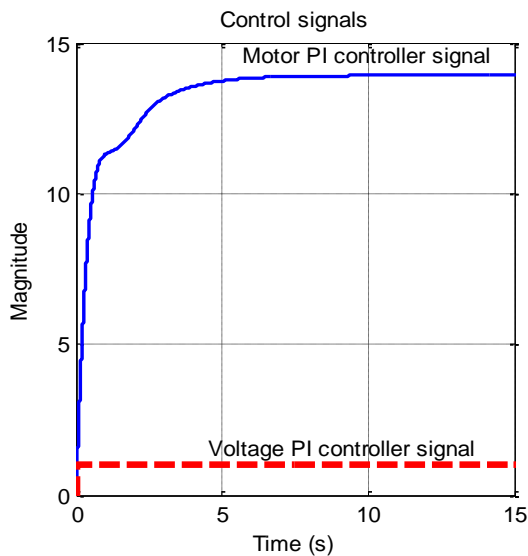


Figure 11(h) Control signal

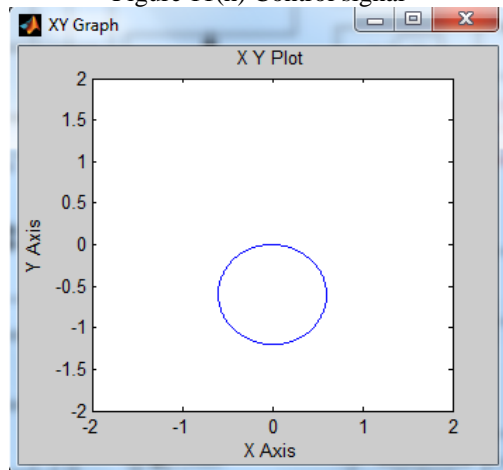


Figure 11(i) Resulted circular motion

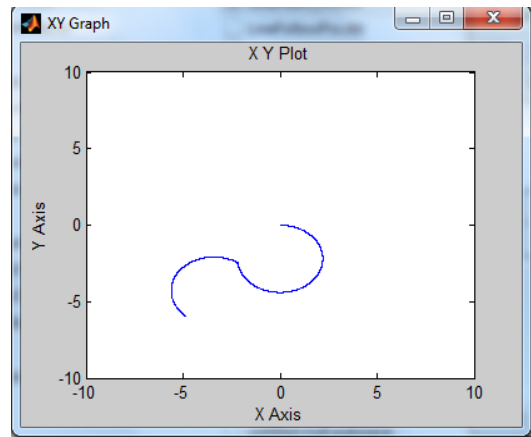


Figure 12 Double curvature motion

Conclusion

A new generalized and refined model for solar electric differential drive Mobile Robotic Platforms (SEDDMRP) and some considerations regarding design, modeling and control solutions are proposed. Each subsystem of the proposed SEDDMRP system's seven main subsystems is mathematically described and corresponding Simulink sub-model is developed, then an integrated generalized model of all subsystems is developed. The proposed model is developed to help in facing the two top challenges in developing Mechatronics SEDDMRP systems; early identifying system level problems and ensuring that all design requirements are met, where it is developed to allow designer to have the maximum output data to select, evaluate, integrate and control the overall SEDDMRP system and each subsystem outputs characteristics and response, for desired overall and/or either subsystem's specific outputs, under various PV subsystem input operating conditions, to meet particular SEDDMRP system requirements and performance. The obtained results of testing the model for straight line, circular and double curvature motions, show the simplicity, accuracy and applicability of the presented models in Mechatronics design of SEDDMRP system application, as well as application in educational process.

Table- 3 Nomenclature and nominal characteristic of SEMRP subsystems

DC machine parameters	
$V_{in}=12\text{ V}$	Input voltage to DC machine
$K_t=1.188\text{ Nm/A}$	Motor torque constant
$R_a = 0.156\ \Omega$	Motor armature Resistance
$L_a=0.82\text{ MH}$	Motor armature Inductance,
$J_m=0.271\text{ kg.m}^2$	Geared-Motor Inertia
$b_m=0.271\text{ N.m.s}$	Viscous damping
$K_b=1.185\text{ rad/s/V}$	Back EMF constant,
$n=1$	Gear ratio
$r=0.075\text{ m}$,	Wheel radius
$J_{equiv}\text{ kg.m}^2$	The total equivalent inertia,
$b_{equiv}\text{ N.m.s}$	The total equivalent damping,
$L=0.4\text{ m}$	The distance between wheels centers
$K_{tac}=1.8\text{ rad/s}$	Tachometer constant,

ω =speed/r, rad/s	=0.5/0.075=6.667 ,also 1/0.075=13.3333
Tshaft	The torque produced by motor
η	The transmission efficiency
Tshaft	The torque, produced by the driving motor
Nominal values for Mobile platform	
M,m, Kg	The mass of the mobile platform
Cd =0.80	Aerodynamic drag coefficient
CL	The coefficient of lift, with values(CL to be 0.10 or 0.16),
Cr=0.5	The rolling resistance coefficient
ρ , kg/m ³	The air density at STP, $\rho =1.25$
a, m/s ²	Platform linear Acceleration
G, m/s ²	The gravity acceleration
N, m/s	The vehicle linear speed.
α , Rad	Road slope or the hill climbing angle
B	Mobile platform's reference area
L	lift,
Af	Platforms frontal area
KP	Proportional gain
KI	Integral gain
Z0	PI controller zero
Pm	The power available in the wheels of the vehicle.
TTotal	The total resistive torque, the torque of all acting forces.
Solar cell parameters	
Isc=8.13 A , 2.55 A , 3.8	The short-circuit current, at reference temp 25°C
I A	The output net current of PV cell (the PV module current)
Iph A	The light-generated photocurrent at the nominal condition (25°C and 1000 W/m ²),
Eg : =1.1	The band gap energy of the semiconductor
$V_t = KT / q$	The thermo voltage of cell. For array :($V_t = N_s KT / q$)
Is ,A	The reverse saturation current of the diode or leakage current of the diode
Rs=0.001 Ohm	The series resistors of the PV cell, it they may be neglected to simplify the analysis.
Rsh=1000 Ohm	The shunt resistors of the PV cell
V	The voltage across the diode, output
q=1.6e-19 C	The electron charge
Bo=1000 W/m ²	The Sun irradiation
$\beta =B=200$ W/m ²	The irradiation on the device surface
Ki=0.0017 A/°C	The cell's short circuit current temperature coefficient

Vo= 30.6/50 V	Open circuit voltage
Ns= 48 , 36	Series connections of cells in the given photovoltaic module
Nm= 1 , 30	Parallel connections of cells in the given photovoltaic module
K=1.38e-23 J/oK; N=1.2	The Boltzmann's constant The diode ideality factor, takes the value between 1 and 2
T= 50 Kelvin	Working temperature of the p-n junction
Tref=273 Kelvin	The nominal reference temperature
Buck converter parameters	
C=300e-6; 40e-6 F	Capacitance
L=225e-6; .64e-6H	Inductance
RI=RL=7e-3	Inductor series DC resistance
rc= RC=100e-3	Capacitor equivalent series resistance, ESR of C ,
Vin= 24 V	Input voltage
R=8.33; 5 Ohm;	Resistance
Ron=1e-3;	Transistor ON resistance
KD=D= 0.5, 0.2,	Duty cycle
Tt=0.1 , 0.005	Low pass Prefilter time constant
VL	Voltage across inductor
IC	Current across Capacitor

References

- [2] Farhan A. Salem, Ahmad A. Mahfouz , A Proposed Approach to Mechatronics Design and Implementation Education-Oriented, Innovative Systems Design and Engineering , Vol.4, No.10, pp 12-39,2013.
- [3] Farhan A. Salem, Dynamic and Kinematic Models and Control for Differential Drive Mobile Robots, International Journal of Current Engineering and Technology , Vol.3, No.2 , pp253-263 (June 2013).
- [4] Farhan A. Salem, Refined modeling and control for Mechatronics design of mobile robotic platforms, Estonian Journal of Engineering, 19, 3, 212–238,2013.
- [5] Farhan A. Salem, Mechatronics motion control design of electric machines for desired deadbeat response specifications, supported and verified by new MATLAB built-in function and Simulink model, European journal, Vol.9, No 36, PP 357:386, 2013.
- [6] Ahmad A. Mahfouz, Ayman A. Aly, Farhan A. Salem , Mechatronics Design of a Mobile Robot System, I.J. Intelligent Systems and Applications, 03, 23-36, 2013.
- [7] Farhan A. Salem, mobile robot dynamics analysis and control ,VI Международная научно-практическая конференция , Moscow, «Инженерные системы - 2013».
- [8] Stephen Se, David Lowe ,Jim Little, Mobile Robot Localization and Mapping with Uncertainty using Scale-Invariant Visual Landmarks, The International Journal of Robotics Research, Vol. 21, No. 8, August 2002, pp. 735-758,2002.

- [9] J. Borenstein, B. Everett, and L. Feng. Navigating Mobile Robots: Systems and Techniques. A. K. Peters Ltd, Wellesley, MA, 1996.
- [10] A.J. Davison and D.W. Murray. Mobile robot localisation using active vision. In *Proceedings of Fifth European Conference on Computer Vision (ECCV'98) Volume II*, pages 809-825, Freiburg, Germany, June 1998.
- [11] J. Borenstein, H.R. Everett, L. Feng, and D. Wehe. Mobile Robot Positioning and Sensors and Techniques, *Invited paper for the Journal of Robotic Systems, Special Issue on Mobile Robots. Vol. 14 No. 4, pp. 231 – 249.*
- [12] Barshan, B. and Durrant-Whyte, H.F., 1995, "Inertial Navigation Systems Mobile Robots." *IEEE Transactions on Robotics and Automation*, Vol. 11, No. 3, June, pp. 328-342.
- [13] PeLoTe Session, Mobile Robots for Search and Rescue, Proceedings of the 2005 IEEE International Workshop on Safety, Security and Rescue Robotics Kobe, Japan, June 2005.
- [14] Bashir M. Y. Nouri, modeling and control of mobile robots, Proceeding of the First International Conference on Modeling, Simulation and Applied Optimization, Sharjah, U.A.E. February 1-3, 2005.
- [15] Ahmad A. Mahfouz, Mohammed M. K., Farhan A. Salem, Modeling, Simulation and Dynamics Analysis Issues of Electric Motor, for Mechatronics Applications, Using Different Approaches and Verification by MATLAB/Simulink (I). *I.J. Intelligent Systems and Applications*, pp. 39-57, 05, 39-57 2013.
- [16] Farhan A. Salem, Modeling and Simulation issues on Photovoltaic systems, for Mechatronics design of solar electric applications, *IPASJ International Journal of Mechanical Engineering (IJME)* Volume 2, Issue 8, August 2014.
- [17] Farhan A. Salem, New generalized Photovoltaic Panel-Converter system model for Mechatronics design of solar electric applications, *International Journal of Scientific & Engineering Research*, Volume 5, Issue 8, August-2014.
- [18] Farhan A. Salem, Photovoltaic-Converter system, modeling and control issues for Mechatronics design of solar electric application, *IJISA*, 2014
- [19] Farhan A. Salem, New generalized and refined Model for Mechatronics design of solar electric mobile robotic platforms, *International Journal of Scientific & Engineering Research*, Volume 5, Issue 8, August-2014
- [20] Emese Sza' Deczky-Krdoss, Ba' Lint Kiss, design and control of a 2-DOF positioning robot *Methods and Models in Automation and Robotics*, Miedzzydroje, Poland, 2004,.
- [21] Gregor Klan'car, Drago Matko, Sa'so Bla'zi'c (2005), Mobile Robot Control on a Reference Path, *Mediterranean Conference on Control and Automation Limassol, Cyprus, June 27-2,.*
- [22] Jose Mireles Jr., Kinematics of Mobile Robots, Selected notes from 'Rob'otica: *Manipuladores y Robots m'oviles'* An'ibal Ollero. 2004
- [23] Julius Maximilian, Kinematics of a car-like mobile robot Mobile robot basic – differential drive", *Institute of Informatics VII, experiment notes*, 2003
- [24] Mircea Ni'ulescu, "solutions for modeling and control in mobile robots", *CEAI*, Vol. 9, No. 3;4, pp. 43-50, 2007, Romania.

Author Profile

Farhan Atallah Salem : Now with Taif University, Mechanical engineering Dept, Mechatronics engineering track.